



SYNTHESIS, CHARACTERIZATION AND SOLAR PHOTOCATALYTIC DEGRADATION OF PHENOL USING DOPED TiO₂ NANOPARTICLES

V.T. Tagad¹, M.E. Navgire¹, G.G. Muley², B.Y. Pagare³, S.K. Narwade³,
A.B. Gambhire^{3,*}

¹Jijamata College of Science and Arts, Bhende, Ahmednagar 414 605, India

²Department of Physics, Sant Gadge Baba Amravati Univeristy, Amravati, 444602, Maharashtra, India

³Department of Chemistry, Shri Anand College of Science, Pathardi, Ahmednagar, 414102, Maharashtra, India

*Corresponding author email: abg_chem@ymail.com

ABSTRACT:

Doped-TiO₂ nanocrystalline powders (*n*M:TiO₂: B, C, N, P, S) with anatase structure were prepared by sol-gel method and characterized by XRD, TEM, XPS, BET surface area, and UV-Vis-DRS. Results revealed that the anatase structure is highly stable for all doped TiO₂ prepared compounds with enhancement in the surface area. UV-Vis diffuse reflectance spectra showed that these dopants were responsible for narrowing the band gap of TiO₂ and shifting its optical response from ultraviolet to visible-light region. The photocatalytic activities of these multi-doped TiO₂ catalysts were investigated by degradation phenol in aqueous solution under solar-light illumination. Under optimization conditions, it was found that C-doped TiO₂ sample shows 97% phenol (0.5 g/l dose) degradation at pH 5.0 and 1 h reaction time as compared to other doped TiO₂ samples, which is ascribed to the enlargement of surface area, lowest crystallite size, light absorption as well as formation of Ti⁺³ which prevent the recombination of electron-hole pairs.

KEYWORDS: Doped-TiO₂; Solar energy; Decomposition of phenol

1. INTRODUCTION

Heterogeneous photocatalysis has received a great deal of attention as an advanced oxidation process for the complete mineralization of organic compounds [1]. However, the development of a practical photocatalytic system focused on the cost effectiveness by the use of renewable solar energy source. Photocatalytic degradation of organic contaminants using solar irradiation could be highly economical compared with the processes using artificial UV-Vis irradiation which required substantial electrical power input. Since phenol is commonly used as a solvent or reagent in industrial processes and chlorophenols are widely used as herbicides and pesticides, research concerning photodegradation of these phenolic pollutants with semiconductor materials has been growing steadily over the last decade [2]. In the present study highly pure and stable anatase multi-doped TiO₂ nanopowders have been prepared by sol-gel method. The synthesized powders were structurally,

morphologically and optically characterized and its photocatalytic properties studies under solar light irradiation.

2. EXPERIMENTAL

B, C, N, P and S doped TiO₂ samples were synthesized using the controlled hydrolysis of titanium butoxide. The dopant starting materials boric acid, mixture of ethylene glycol and citric acid, ammonia, ortho-phosphoric acid and thiourea were used for the preparation of the samples, respectively. In a typical experiment, 0.1 mol of titanium butoxide was dissolved in 100 ml anhydrous ethanol to form solution. A certain amount of boric acid, ethylene glycol and citric acid, ammonia, ortho-phosphoric acid and thiourea were dissolved in a mixture of 50 ml deionized water containing 2 ml nitric acid and 50 ml of ethanol separately. To this, TiO₂ solution was added drop-wise under vigorous stirring to form the precipitate by simultaneous addition of ammonium hydroxide pH at 7 (excluding N-doped TiO₂ solution). After keeping

the precipitate for aging (5 days), it was concentrated and dried. The samples, after overnight drying at 110°C, were calcined for 2 h at 500°C.

3. RESULTS AND DISCUSSION

3.1 XRD Analysis

Fig. 1 shows the XRD patterns of the pure TiO₂ and *n*M:TiO₂ samples, respectively. Pure TiO₂ shows two main peaks at 2θ =25.4 and 27.5, corresponding to (101) phase of anatase and (110) phase of rutile, respectively.

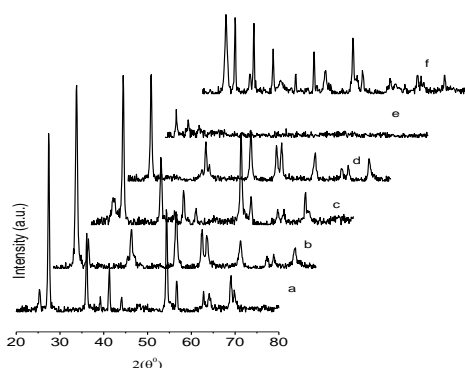


Fig. 1(a-f). XRD profiles of (a) pure TiO₂ (b) B-TiO₂ (c) C-TiO₂ (d) N-TiO₂ (e) P-TiO₂, and (f) S-TiO₂, calcined at 500°C.

In the case of multi-doped TiO₂ (Fig. 1(b-k)), the rutile phase is < 3%, which means multi-doping retards the transformation from anatase to rutile phase. Multi-doping of the TiO₂ stabilizes a well-crystallized pure anatase upon calcination at 500°C, in contrast with the simultaneous growth of the rutile phase observed for the pure TiO₂. The particle size calculated from XRD data is as large as 15-25 nm for B, P, S and as small as 10-13 nm for the C and N doped TiO₂.

2.2. TEM analysis

In order to further confirm the effect of metal and non-metal doped samples on particle size and hence higher specific surface area of composite powder, the particle size N-TiO₂ and C-TiO₂ were observed using TEM. Fig. 2(a-c) shows TEM images N-TiO₂ and C-TiO₂, respectively and its corresponding Fourier transfer patterns (FTT) are also presented in the inset of figures. It can be seen that the particle size of composite powders are about 10-15 nm.

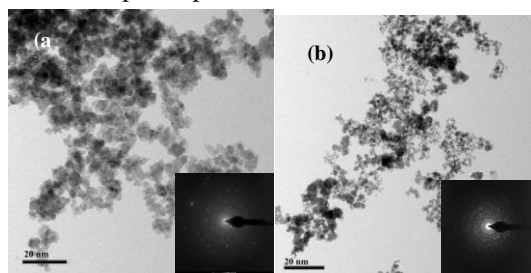


Fig. 2(a-b). The TEM images of (a) N-TiO₂ (b) C-TiO₂.

3.2. UV-vis DR spectral analysis

UV-Vis diffuse reflectance spectroscopy (Fig. 3(a-k)) permits the detection of framework of TiO₂ in the samples. In all the samples, characteristic band for tetrahedrally coordinated titanium appears at about 350 nm. A progressive red-shift in the band-gap absorption is noticed with non-metal loading than that of pure TiO₂ (Fig. 3(a)). However, the edges of the absorption of the non-metal ion doped samples were shifted to approximately 500 nm, corresponding to band-gap energy of 2.11 eV. The absorption onsets were determined by linear extrapolation from the inflection point of the curve to the baseline.

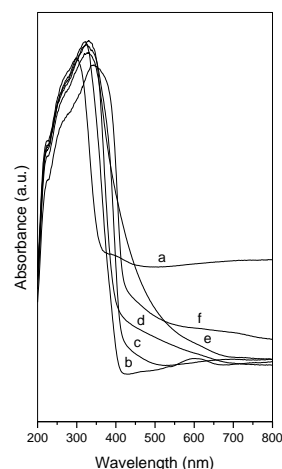


Fig. 3(a-f). UV-Vis-DR spectra of (a) pure TiO₂ (b) S-TiO₂ (c) B-TiO₂ (d) P-TiO₂ (e) N-TiO₂, and (f) C-TiO₂.

3.3. XPS studies

Fig. 4. shows Ti2p XPS spectra of the C-TiO₂. The Ti2p level shows asymmetry toward the lower binding energy side.

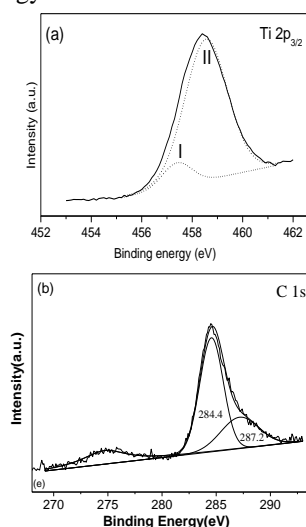


Fig. 4. High resolution XPS spectra of C-TiO₂.

The peaks are resolved into two components, with binding energy values of 457.5 and 458.6 eV for the first and second components, respectively. These

binding energies are well matching with the binding energy values of Ti_2O_3 and TiO_2 [3]. The binding energies and spin orbital splitting (difference between binding energy of $Ti2p_{3/2}$ and $Ti2p_{1/2}$) is well matching with reported values of Ti_2O_3 and TiO_2 . The formation of Ti_2O_3 might be due to the reduction in residual carbon in the layer from organic radicals. The carbon produced in decomposition of organic radicals during thermal treatment at $500^\circ C$ draws oxygen from the surrounding atmosphere, which causes a reduction in some Ti (IV) to Ti (III) species. The C 1s spectra of the sample shared two peaks at around 284.4 and 287.2 eV binding energy. The 284.4 eV peak is due to carbon-containing species adsorbed on the surface, and the 287.2 eV peak indicates the presence of C-O bonds [4].

3.4. Photocatalytic activity

The photocatalytic degradation of phenol was performed taking 0.01 g/l of phenol in water and 0.6 g/l of catalyst. The solutions were exposed to sunlight in closed pyrex flasks at room temperature with constant stirring. All the experiment were carried out during summer days from 12:00 AM to 1:00 PM. The photocatalytic activities of pure TiO_2 , nM: TiO_2 samples are shown in Fig. 5.

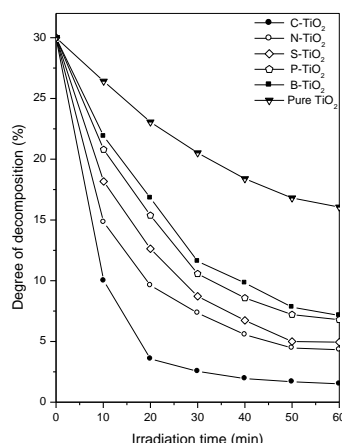


Fig. 5. Rate of decomposition of phenol by using (a) pure TiO_2 , (b) B- TiO_2 (c) C- TiO_2 (d) N- TiO_2 (e) P- TiO_2 , and (f) S- TiO_2 , calcined at $500^\circ C$.

In the presence of pure TiO_2 , decomposition of Phenol was not observed. However, in the presence of the non-metal doped TiO_2 samples, the decomposition of phenol obviously increase. Among the different non-metal incorporated samples, C- TiO_2 sample exhibited the highest photocatalytic activity under solar light irradiation, only 5-7% of phenol remained, and in the case of N 10% of phenol remained after exposure to solar light for 60 min. While as high as 20-25% remained in the case of B, P, and S doped TiO_2 . From the observed results it was found that the C- TiO_2 sample is found

to be composite photocatalyst, in this case once optical excitation occurs, the photogenerated electrons can be transferred to the lower-lying conduction bands of carbon while the holes will accumulate in the valance band of TiO_2 , effectively scavenged by the oxidation of phenol, whereas the photogenerated electrons can be transferred into the surface of carbon rather than undergoing bulk recombination. The carbon in C- TiO_2 reduces TiO_2 to form Ti^{+3} ions. Ti^{+3} can trap photogenerated electrons in the conduction band and prevent the recombination of electron-hole pairs under solar light illumination. Moreover, nM: TiO_2 samples shows red-shift in the absorption range compared with pure TiO_2 . The existence of oxygen deficiencies, probably located at the anatase-rutile boundary, leads to localized electronic states between the valence and conduction band, shows certain absorption in the visible range. This seems to indicate the absorption could also enhance the efficiency of the photocatalytic reaction since the number of photons participating in the photocatalytic reaction is larger.

4. Conclusion

Multi-doped TiO_2 nanoparticles were successfully prepared by a sol-gel method. It was found that the prepared photocatalyst exhibited smaller shape particles and higher specific surface area. In addition to oxides of Ti^{+4} , there was a certain amount of Ti^{+3} oxides existed. The absorption edge of metal and non-metal doped TiO_2 exhibited significant red shift to visible region. The high photocatalytic activity of the C- TiO_2 under solar light irradiation can be attributed to small particle size, high specific surface area, optical absorption and displayed photocatalytic activity in the visible region.

References

- [1]. T. Oyama, A. Aoshima, S. Horikoshi, H. Hidaka, J. Zhao, N. Serpone, Sol. Energy Mater. Sol. Cells., 2004, 94, 327-331.
- [2]. S. Chatterjee, S. Sarkar, S.N. Bhattacharya, J. Photochem. Photobiol. A: Chem. 1994, 81, 199-203.
- [3]. J. Yu, X. Zhao, Mater. Res. Bull., 2001, 36, 97-101.
- [4]. W. Ren, Z. Ai, F. Jia, L. Zhang, X. Fan, Z. Zou, Appl. Catal. B: Environ., 2007, 69, 138-41.